ACS APPLIED MATERIALS & INTERFACES

Research Article

www.acsami.org

Grafting Hyaluronic Acid onto Gold Surface to Achieve Low Protein Fouling in Surface Plasmon Resonance Biosensors

Xia Liu,[†] Renliang Huang,*[,‡] Rongxin Su,*[,†,§] Wei Qi,[†,§] Libing Wang,[†] and Zhimin He[†]

[†]State Key Laboratory of Chemical Engineering, School of Chemical Engineering and Technology, and [‡]School of Environmental Science and Engineering, Tianjin University, Tianjin 300072, People's Republic of China

[§]Collaborative Innovation Center of Chemical Science and Engineering (Tianjin), Tianjin 300072, People's Republic of China

Supporting Information

ABSTRACT: Antifouling surfaces capable of reducing nonspecific protein adsorption from natural complex media are highly desirable in surface plasmon resonance (SPR) biosensors. A new protein-resistant surface made through the chemical grafting of easily available hyaluronic acid (HA) onto gold (Au) substrate demonstrates excellent antifouling performance against protein adsorption. AFM images showed the uniform HA layer with a thickness of ~10.5 nm on the Au surface. The water contact angles of Au surfaces decreased from 103° to 12° with the covalent attachment of a carboxylated HA matrix, indicating its high hydrophilicity mainly resulted from carboxyl and amide groups in the HA chains. Using SPR spectroscopy to investigate nonspecific adsorption from single protein solutions (bovine serum albumin (BSA), lysozyme) and complex media (soybean milk, cow milk, orange juice) to an HA matrix, it was found that ultralow or low protein adsorptions of 0.6−16.1 ng/cm^2 (e.g., soybean milk: 0.6 ng/cm^2) were achieved on HA-Au surfaces. Moreover, anti-BSA was chosen as a model recognition molecule to characterize the immobilization capacity and the antifouling performance of anti-BSA/HA surfaces. The results showed that anti-BSA/HA sensor surfaces have a high anti-BSA loading of 780 ng/cm^2, together with achieving the ultralow (<3 ng/cm^2 for lysozyme and soybean milk) or low (<17 ng/cm^2 for cow milk and 10% blood serum) protein adsorptions. Additionally, the sensor chips also exhibited a high sensitivity to BSA over a wide range of concentrations from 15 to 700 nM. Our results demonstrate a promising antifouling surface using extremely hydrophilic HA as matrix to resist nonspecific adsorption from complex media in SPR biosensors.

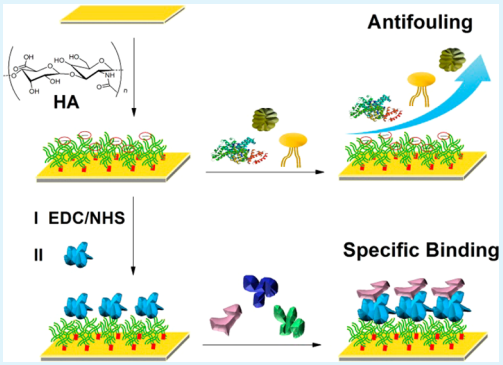

KEYWORDS: *SPR, hyaluronic acid, antifouling, nonspecific adsorption, biosensor*

INTRODUCTION

Surface plasmon resonance (SPR) biosensor, as a powerful tool for monitoring molecular interactions, has been widely used in the field of pharmaceutics, diagnostics, food safety, and environmental monitoring.[1−5] During the SPR analysis, surface fouling of sensor chips is a ubiquitous and problematic phenomenon that can reduce the accuracy of quantitative results. Protein fouling referred to as nonspecific adsorption from natural samples (e.g., blood, milk, juice, sanitary sewage) is a crucial issue for SPR sensing because the target can be determined accurately only in the presence of a protein-resistant background.[6,7] For example, the cellular components of a blood sample still contain 60−80 g/L protein complex; then they could adsorb nonspecifically to the SPR sensor chips and generate a high noise signal to prevent the detection of target analytes with low concentrations (down to ng/L).[8−10] Therefore, it is highly desirable to design and fabricate a protein-resistant surface that is capable of reducing or ideally eliminating nonspecific adsorption of proteins to improve the SPR sensitivity and accuracy in the measurement of natural samples.

Surface hydration is generally believed to be the dominant factor in preventing nonspecific adsorption of proteins. Many hydrophilic materials, such as poly(ethylene oxide),[7] oligo (ethylene glycol),[11−14] polydopamine/polymers,[15,16] saccharides,[17−19] and poly(β-peptoid)s,[20,21] have been employed to fabricate nonfouling surfaces via hydrogen bond-induced hydration. Pop-Georgievski et al.[7] reported a poly(ethylene oxide) grafted surface with low protein adsorption of 7 ng/cm^2 from human blood plasma. Lin et al.[20] demonstrated that poly(β-peptoid)s could reduce the adsorption of proteins from 100% plasma to 9.8 ng/cm^2. The strong proton-accepting ability of poly(β-peptoid)s was considered as a key factor for forming hydrogen bonds with water and thus increasing the strength of hydration. On the other hand, zwitterionic polymers, such as poly(carboxybetaine) (pCB),[22] poly(sulfobetaine) (pSB),[23] and polyampholytes,[24] were designed and synthesized to prevent protein adsorption because of their strong hydration capacity via electrostatic interactions. In this

Received: May 13, 2014
Accepted: July 5, 2014
Published: July 15, 2014

respect, Jiang and co-workers developed many pCB-and pSB-based zwitterionic polymers that demonstrated ultralow fouling in complex media.[6,22,23,25−27] For example, a two-layered polycarboxybetaine acrylamide binding platform was designed to achieve both ultralow protein fouling (<5 ng/cm^2 from undiluted blood plasma) and high immobilization capacity of recognition molecules.[27] Additionally, Vaisocherová etal.[28] also demonstrated that poly(carboxybetaine acrylamide) had the low adsorption capacity (<10 ng/cm^2) from undiluted biological media, such as cow milk, tomato, and orange juice. The amphiphilic copolymers with alternation of hydrophilic and hydrophobic domains could also be employed to reduce the nonspecific adsorption.[29,30] Overall, these rationally designed and synthetic materials exhibited good antifouling performance against protein adsorption. Nonetheless, for SPR sensing, an ideal antifouling material also required high stability, high immobilization capacity, and excellent compatibility to recognition molecules, as well as low cost and facile fabrication. It is still difficult for a single system to satisfy all of the above-mentioned requirements. The design of new protein-resistant SPR sensor chips with commercial potential has attracted extensive attention in recent years.

Polysaccharides, as a class of natural hydrophilic macromolecules, have been used in biosensors, biotechnology, and biomedicine, due to their high stability, excellent compatibility to bioactive agents, and easy availability and functionalization.[17,31,32] A classic example is the use of carboxylated dextran as matrix to fabricate SPR sensor chips, which had been commercialized under the trade name of CM by GE Healthcare, Biacore. However, previous studies had demonstrated that carboxylated dextran itself cannot effectively prevent protein adsorption from complex samples and thus needs further modification such as zwitteration with carboxybetaine.[17,32] In view of the structural diversity of polysaccharides, this study aims to design and fabricate a new protein-resistant surface using natural polysaccharide as an alternative of dextran for SPR biosensors.

Among various polysaccharides, hyaluronic acid (HA) has received great attention in medical and cosmetic applications. As an anionic glycosaminoglycan, HA possesses superior inert property as compared to other polysaccharides and exhibited high antifouling stability (against fibronectin adsorption) that was evidenced by treatment with phosphate buffer saline (PBS) solution for 7 days.[33,34] Different from dextran, the disaccharide unit in HA molecules has amide (CO−NH) and carboxy (COOH) groups, which provide hydrogen-bond donor/acceptor and thus enhance the hydration strength, creating a repulsive force on proteins.[35] These chemical groups also existed in synthetic polypeptide and zwitterionic polymers with excellent protein antifouling ability.[20−22] On the basis of this unique structure, we expect HA to be a promising protein-resistant material with better performance than dextran. Recently, Bauer et al.[36] investigated the nonfouling properties of HA and hydrophobic trifluoroethylamine-modified HA (TFEA-HA) against marine fouling organisms. The results indicated that both HA and TFEA-HA grafted glass surfaces could reduce the adhesion strength of marine organisms such as bacterium (*Cobetia marina*), seaweed (*Ulva linza*), and diatom (*Navicula incerta*). This further verifies our speculation, and we are the first to report utilization of HA for the construction of SPR sensor chips with good antifouling performance against protein adsorption.

In this study, we design and fabricate HA-based SPR sensor chip through grafting HA molecules onto a gold (Au) surface. The grafting process was monitored by SPR spectroscopy to ensure successful chemical binding of HA to the Au surface. The resulting HA-Au chips were further characterized using contact angle (CA) measurements and atomic force microscopy (AFM). We then investigated the protein-resistant performance of HA-based surfaces by SPR spectroscopy using single protein (lysozyme, BSA) and natural protein-containing complexes (cow milk, soybean milk, orange juice) as test samples. Meanwhile, we chose the anti-BSA/BSA interaction as a typical model to verify the feasibility in quantitative determination of target analytes. The immobilization capacity of anti-BSA onto HA-Au surface, as well as the antifouling performance of antibody-immobilized HA surface, were also investigated as part of our study.

EXPERIMENTAL SECTION

Materials. Two types of HA extracted from rooster comb with molecular weight of 1000 and 350 kDa were obtained from Sigma-Aldrich and Heowns Business License (China), respectively. 1-Ethyl-3-(3-(dimethylamino)propyl)-carbodiimide hydrochloride (EDC) and *N*-hydroxysulfosuccinimide (NHS), 11-mercapto-1-undecanol (MUO), epoxy chloropropane (EC), 2-morpholino-ethanesulfonic acid (MES), ethanolamine hydrochloride (EA), bromoacetic acid, bis(2-methoxy ethyl) ether, lysozyme, bovine serum albumin (BSA), and dextran (MW: 100 kDa) were purchased from Sigma-Aldrich and used immediately upon receipt. BSA antibodies (anti-BSA) were obtained from Abcam (U.S.). Cow milk with a protein concentration of about 30 mg/mL was from Yili Industrial Co. and purchased in a local market. Blood serum was obtained from BEST-Biotech, Inc. (China).

Bare Au Pretreatment. BK7 glass substrates were deposited with a 2 nm chromium adhesion-promoting layer followed by a 50 nm gold layer using an electron beam evaporator (10 kV Temescal Series 260 E-beam Source) at a base pressure of 10^{-6} Torr. The deposition rates for chromium and gold were 0.5 and 1 Å/s, respectively. The resulting bare gold chips were cleaned by immersion in freshly prepared "piranha" solution (3:7 mixture of 30% H_2O_2 and concentrated H_2SO_4) for 3 h at room temperature. The piranha-treated bare Au chips then were rinsed with anhydrous ethanol and deionized water, followed by drying with compressed nitrogen. The pretreated Au chips were then stored in an enclosed container at −4 °C for subsequent use.

Fabrication of HA-Au Chips. The cleaned and dried bare Au chips were initially immersed in an ethanol solution of 11-mercapto-1-undecanol (MUO, 10 mM) for 12 h at 25 °C, forming a self-assembled monolayer (SAM) tailed with hydroxyl groups onto Au surfaces. Next, the SAM-Au chips were immersed in a bis(2-methoxy ethyl) ether solution of epoxy chloropropane (0.6 M) for 4 h at 25 °C, followed by immersing in an aqueous solution (0.1 M NaOH) of HA (1000 kDa, 3 mg/mL) for 20 h at 25 °C. The resulting HA coated Au chips (HA_0-Au) were then carboxylated with an aqueous solution (0.1 M NaOH) of bromoacetic acid (0.1 M) for 16 h at 25 °C. The carboxylated HA coated Au chips (HA-Au) were then rinsed thoroughly with anhydrous ethanol, dried with nitrogen, and stored in an enclosed container at −4 °C for further use.

To make a comparative analysis, HA with MW 350 kDa and dextran with MW 100 kDa were also employed to modify bare Au chips following the procedure as mentioned above. The concentrations of HA and dextran were 3 and 10 mg/mL, respectively, while all other conditions were the same as given previously. The default molecular weight of HA used in this work is 1000 kDa unless otherwise noted.

Surface Characterization. To monitor the fabrication of HA-Au chips, angle-scanning SPR spectroscopy was employed to determine the angle shift of different chips (bare Au, SAM, Epo-Au, HA_0-Au, to HA-Au). Phosphate-buffered saline (PBS, containing 10 mM

phosphate, 138 mM sodium chloride, and 2.7 mM potassium chloride, pH 7.4) was used as running buffer to conduct experiments.

The static contact angles were measured with a contact angle measuring device OCA15EC (DataPhysics Instruments, Germany) equipped with SCA 202 software. One microliter water drops were deposited on tested surfaces, and the data were collected. The contact angle was calculated by numerical curve fitting of the droplet profile at the three-phase boundary from the image captured by a CCD camera. Reported values are averages of four measurements recorded at different positions on each substrate. All measurements were performed under ambient conditions with relative humidity ~50%.

The surface topography of bare Au and HA-Au chips was characterized by atomic force microscopy in a contact mode using an AFM 5500 (Agilent, U.S.) equipped with N9797 AU-1FP Pico software. Commercial silicon nitride probes (NP-S, Bruker AFM Probes, U.S.) with an elastic modulus of 0.58 N/m were used to perform the experiments. The thickness of the HA layer was determined as the distance between the top of the HA layer and the uncovered gold substrate by scratching the HA layer.

Measurements of Nonspecific Protein Adsorption by SPR. To assess the protein-resistant performance, we used five different protein samples including two single protein solutions and five natural complex media. Specifically, lysozyme and BSA were dissolved in a PBS (as above) solution to a final concentration of 1 mg/mL, respectively. Soybean milk was prepared by milling the commercial soybean with deionized water to a final protein concentration of about 10 mg/mL. Orange juice was prepared by directly milling the fresh orange without the addition of water, giving rise to a protein concentration of 10 mg/mL. Cow milk, 10% blood serum, and 100% blood serum were used without dilution. All of the natural samples were centrifuged three times (20 min/time) at 5000 rpm (Sigma 3-18K, Germany) followed by filtration through a 0.22 μm filter (Millex-GP, Millipore, U.S.).

A time-resolved surface plasmon resonance (TR-SPR) spectrometer (DyneChem HiTech Ltd., Changchun, China), which is a single channel and prism coupling-based instrument equipped with a 650 nm laser as the light source, was employed to monitor the real-time nonspecific protein adsorption onto HA or anti-BSA immobilized HA surfaces. A baseline signal was established by applying a PBS buffer solution at a flow rate of 50 μL/min over the chips' surface for about 30 min. The protein-containing solutions were injected into the flow cell at a flow rate of 10 μL/min for 10 min (or 20 min for BSA) followed by a cleaning with PBS solution for 10 min (or 5 min for BSA), leading to the SPR angle shift recorded as $\Delta\theta$ values in the SPR system. Especially, to directly observe this angle shift, we also performed the angle scanning over a range of 57°−72° before protein injection and after PBS washing. According to the results in previous studies[37] and to the recommended calculation method in the commercial instruments (e.g., Thermo FT-SPR, BioNavis MP-SPR), 0.1°−0.15° angle shift was used to represent a surface coverage of 100 ng/cm^2. On the basis of the TR-SPR system, a shift in SPR angle of 0.12° corresponds to a surface coverage of 100 ng/cm^2. The former value was estimated by comparing the infrared reflection−absorption spectroscopy by a known amount of BSA deposited on the SPR chips.[7]

Quantitative Determination of BSA by SPR. To immobilize anti-BSA molecules, the carboxyl groups of HA-Au chips were activated in an MES (pH 6.0, containing 0.1 M MES and 0.5 M NaCl) solution of 0.4 M EDC and 0.1 M NHS for 15 min. The activated HA-Au chips were rinsed immediately with Milli-Q water, immersed in a PBS solution of anti-BSA (1 mg/mL) for 30 min at 25 °C, and then washed thoroughly with PBS solution. The residual NHS-activated carboxyl groups were deactivated by ethanolamine solution (1 M, pH 8.0) for 7 min. SPR angle shift was measured before and after anti-BSA binding to calculate the immobilization capacity of HA-Au chips.

The anti-BSA loaded HA-Au chips were fixed in the SPR set to characterize the interaction between anti-BSA and BSA by recording the real-time angle shift ($\Delta\theta$) values in the SPR system. A steady baseline was established by flowing PBS buffer solution at a flow rate of 50 μL/min. The BSA solutions with different concentrations (from 0.12 nM to 2.3 μM), such as 15, 75, 150, 300, 450, and 700 nM, were injected respectively into the flow cell at a flow rate of 30 μL/min for 3 min followed by washing with PBS solution. To detect the BSA with different concentrations, we regenerated the sensor chips using 10 mM NaOH solution until the SPR signal was back to baseline.

RESULTS AND DISCUSSION

Fabrication and Characterization of HA-Au Chips. Scheme 1 illustrated the strategy for grafting HA onto Au substrates. In this process, the bare Au chips were functionalized initially with 11-mercapto-1-undecanol ($HS(CH2)_{11}OH$) via Au-SH interactions, leading to the formation of SAM and hydroxylated Au surfaces. We then derivatized the SAM via the activation of hydroxyl groups with epoxy chloropropane, forming activated SAM with epoxy groups on Au substrates (Epo-Au). Covalent attachment of HA onto Au surface (HA_0-Au) was accomplished via ring-opening reactions between epoxy and hydroxyl groups under basic condition. Finally, the resulting HA_0-Au chips were carboxylated with bromoacetic acid (CH_3COOBr) to obtain a negatively charged HA layer on Au surfaces (HA-Au).

Scheme 1. Schematic Illustration of Grafting HA Molecules to Bare Au Surfaces

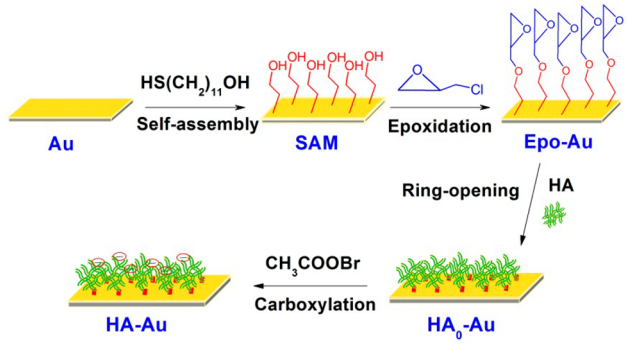

To monitor the grafting process, we employed SPR spectroscopy to measure the change in the SPR angle because of its high sensitivity to surface modifications. As shown in Figure 1, the bare Au chip has an SPR angle of 61.805°, which was shifted to 62.030° after modification with hydroxyl-tailed

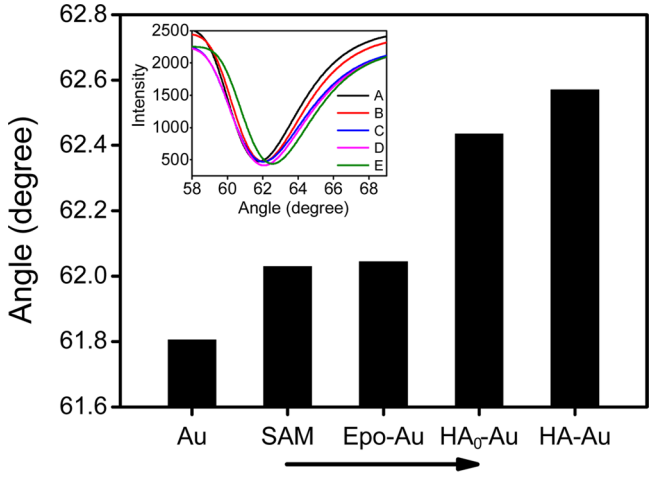

Figure 1. Shift in SPR angle during the grafting process from bare Au to HA-Au chips. The inset figure shows the angle scanning spectra corresponding to each state of sensor chips.

SAM. The increase in SPR angle provided direct evidence of the successful modification with SAM. Further grafting with epoxy chloropropane (EC) led to a small SPR angle shift (0.015°) probably because there was not 100% conversion of the SAM and/or the RIs of the materials are dissimilar. A significant increase in SPR angle from 62.045° to 62.435°, which corresponded to approximately 325 ng/cm^2 (0.12° ≈ 100 ng/cm^2), was observed after the grafting of HA to Au surfaces (HA_0-Au), leading us to believe that the large molecular weight of HA (1000 kDa) is an important attribute in the SPR angle shift. After the carboxylation reaction, the SPR angle further increased to 62.571°, which is slightly larger than that of HA_0-Au and may be related to a large content of carboxyl groups. During the modification process from bare Au to HA-Au surfaces, the SPR angle shift was about 0.766°, suggesting the successful grafting of a thin HA layer on Au surfaces. No significant change in the SPR angle was found after washing with ethanol, drying with nitrogen, rewetting with PBS solution, and continuous use for more than 24 h in PBS solution (data not shown), indicating high stability of the covalently grafted HA layer.

To characterize the hydrophilicity of HA-Au surfaces, we measured the static water contact angles of unmodified Au, SAM, and HA-Au substrates. As shown in Figure 2 and

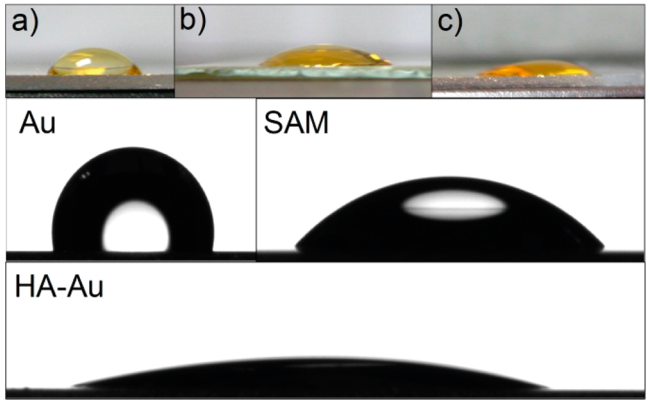

Figure 2. Photographs and contact angles images of the bare Au (a), SAM (b), and HA-Au (c) surfaces.

Supporting Information Table S1, bare Au without any pretreatment was highly hydrophobic (103°), while SAM coated Au surfaces exhibited slight hydrophilicity with a contact angle of 46°, presumably due to the influence of the hydroxyl groups. As expected, the HA-grafted Au substrates led to a lower contact angle (12°, Supporting Information Table S1) and displayed extreme hydrophilicity. The contact angle of HA-Au surface is near the reported values of other antifouling materials in the literature, such as zwitterionic polymer (e.g., poly-MEDSAH, 12°;[38] poly-MPDSAH, 17°[39]), poly(β-peptoid)s (17°),[20] and poly(ethylene oxide) (9°).[7]

To further directly observe the surface morphology of bare Au and HA-Au chips, we employed atomic force microscopy (AFM) to characterize the dried samples. Figure 3 shows typical AFM images of Au surfaces before and after the grafting of HA. The dried HA layer (Figure 3d) had larger uniform hills distributed on the gold surface as compared to the bare Au surfaces (Figure 3b). These nanosized HA hills probably resulted from the dry-induced aggregation of the HA chains. To confirm this speculation, we employed liquid-AFM analysis to observe the real surface morphology of the HA-Au chip in the wet state (in PBS buffer). As shown in Figure 3e,f, the HA-Au chip in the wet state has a smooth surface with an rms roughness of 0.4 nm, which was much lower than that of the bare Au surface (8.36 nm), indicating the formation of a uniform HA layer on Au surface. Furthermore, we employed AFM to measure the height difference between HA layer and the glass surface by scratching. As shown in Supporting Information Figure S1, the thickness of the HA layer that completely covered the Au surface is calculated as 10.5 nm.

Nonspecific Protein Adsorption on HA Surfaces. As we know, SPR spectroscopy is highly sensitive to surface adsorbates and has a practical detection limit of approximately 1 ng/cm^2.[20,40] In this study, the angle resolution of TR-SPR system is 0.0015°, which corresponds to 1.25 ng/cm^2. To assess the antifouling ability of as-prepared surfaces, we employed SPR spectroscopy to detect the nonspecific adsorption using bovine serum albumin (BSA) as a model protein. In a typical experiment, the SPR chips (bare Au, SAM, dextran-Au, HA_0-Au, or HA-Au) were exposed to PBS buffer to establish a stable baseline. An aqueous solution containing 1 mg/mL BSA was then passed over the surface at a flow rate of 10 μL/min for 20 min. Next, the chip was exposed a second time to the PBS buffer. Figure 4a shows the real-time SPR signal (angle shift, $\Delta\theta$) resulting from BSA adsorption and desorption. For the bare Au chip, the SPR angle increased immediately after the injection of BSA. After PBS washing for 20 min, a large SPR response denoted as angle shift ($\Delta\theta$) was still observed. These results provide direct evidence in support of a large amount of BSA adsorption onto the Au surface, and point out the difficulty of protein desorption. As shown in Figure 4a, SAM modification could significantly reduce protein adsorption, which we observed as lower angle shift, due to the improvement of surface hydrophilicity. Further grafting of dextran or HA onto Au surface led to fewer BSA adsorbed on such chips.

To directly observe the SPR angle shift, the angle scanning was carried out before BSA injection and after PBS washing. As shown in Supporting Information Figure S2, the results were in agreement with that from real-time SPR analysis. A significant angle shift (0.315°) for bare Au surface could be observed in Supporting Information Figure S2a, while similar SPR spectra were obtained for dextran and HA grafted sensor chips. To test further stablility, we stored the HA-Au chips in an enclosed container for 4 months (dried state) and in PBS solution for a week (wet state), respectively. These chips also showed a very low $\Delta\theta$ shift similar to those before storage for BSA adsorption, indicating a high antifouling stability of HA matrix.

In general, we observed the mass of the adsorbed protein is approximately proportional to the angle shift within a narrow range of SPR angle. A 0.12° angle shift corresponds to 100 ng/cm^2 of surface coverage for our SPR system (see the Experimental Section). Figure 4b summarizes the nonspecific adsorption of BSA on different surfaces. The bare Au surface had a high adsorption of 262 ng/cm^2, while the HA-Au surface can effectively resist BSA adsorption down to a level of 7.7 ng/cm^2, which is much lower than that on dextran-Au (15.4 ng/cm^2) and SAM (59.6 ng/cm^2) surfaces. Similar BSA adsorptions could also be obtained using original HA before carboxylation (HA_0-Au, 9.2 ng/cm^2) and HA with lower molecular weight of 350 kDa (8.0 ng/cm^2). In fact, some of the adsorption values for HA-Au chips are below or close to the detection limit of SPR (1.25 ng/cm^2). In comparison with dextran, HA has a better antifouling performance presumably

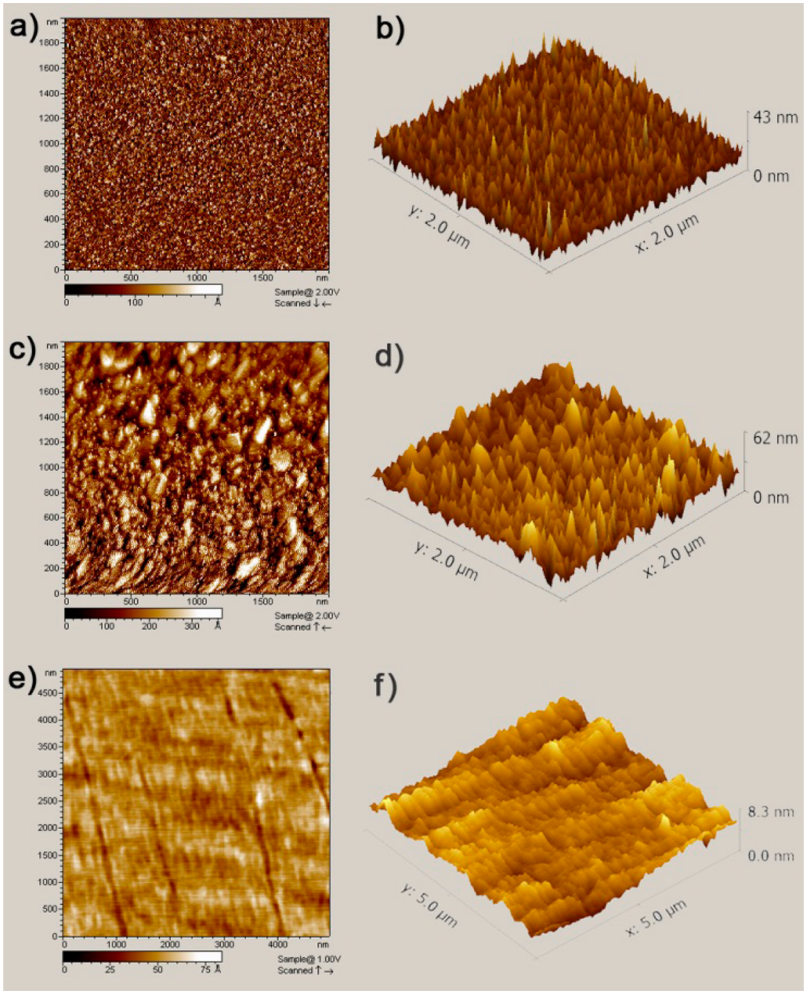

Figure 3. Flattened and topographic AFM images of bare Au (a,b) and HA-Au surface in the dry state (c,d) and the HA-Au surface in the wet state (e,f).

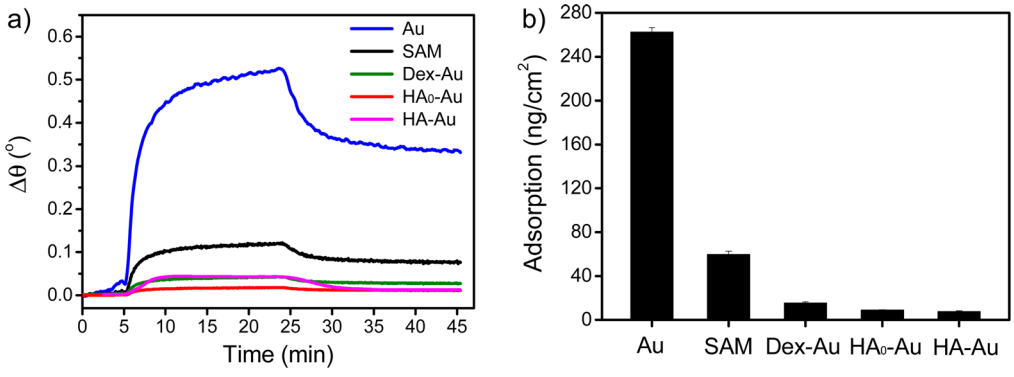

Figure 4. (a) SPR sensorgrams showing the nonspecific protein adsorption onto bare Au, SAM, dextran-Au (dex-Au), HA_0-Au, and HA-Au surfaces. (b) The amount of nonspecific protein adsorption to various surfaces. Each error bar represents the standard deviation from three independent experiments.

due to higher content of hydrophilic groups, such as COOH, CO−NH, and OH, which enable HA to have a stronger hydration capacity. In addition, it is easier for amide (CO−NH) group present in HA to form hydrogen bonds than for the hydroxyl (OH) groups in dextran.[41] Although the protein-resistant performance of HA layer is slightly poorer than that of the typical zwitterionic polymer (<5 ng/cm^2)[22] or poly(β-peptoid)s (<5 ng/cm^2),[20] the high stability, excellent compatibility, easy availability, and low cost of HA allow it to become a potential new antifouling material for SPR biosensors.

Another typical protein, lysozyme (MW = 14.7 kDa, pI = 11), was also used to characterize the protein-resistant performance of HA-Au chips. The real-time SPR response (angle shift, $\Delta\theta$) and SPR angle scanning spectra before and after lysozyme adsorption were shown in Supporting

Information Figures S3a and S4a, respectively. In this case, the nonspecific protein adsorption on HA-Au surface was 4.6 ng/cm^2 (Figure 5a), which is below the commonly accepted ultralow fouling criteria of <5 ng/cm^2 and similar to the reported values of synthetic antifouling materials.[20,22,42,43]

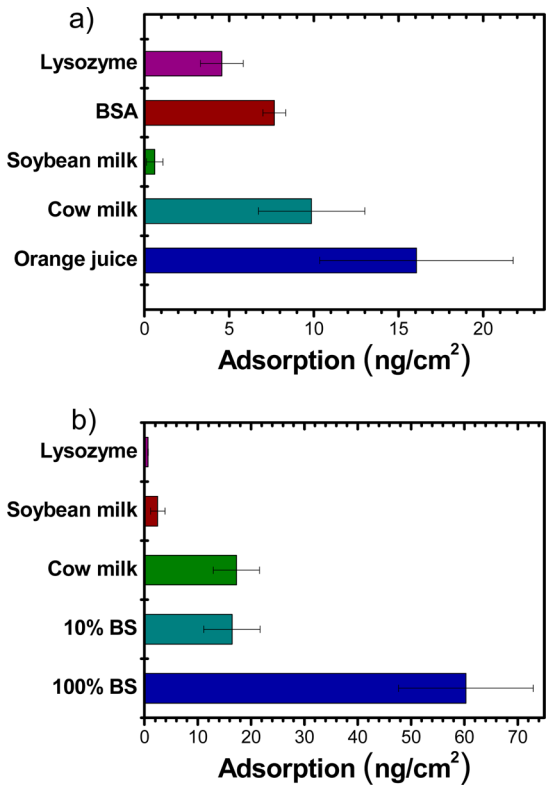

Figure 5. Protein nonspecific adsorption from single protein solutions (lysozyme, 1 mg/mL; BSA, 1 mg/mL) and natural complex media (soybean milk, ~10 mg/mL; cow milk, ~30 mg/mL; undiluted orange juice, ~10 mg/mL) on HA-Au surface. (b) The amount of nonspecific protein adsorption from several solutions (lysozyme, soybean milk, cow milk, 10% blood serum, 100% blood serum) to anti-BSA immobilized HA-Au surfaces. Each error bar represents the standard deviation from three independent experiments.

The good protein-resistant performance against single protein adsorption prompted us to evaluate the antifouling property of HA-Au chips in protein complex-containing natural food media, including soybean milk (~10 mg protein/mL), cow milk (~30 mg protein/mL), and undiluted orange juice (~10 mg protein/mL). These food-safety related samples contain protein, carbohydrate, fat, vitamin, etc., making for more challenging media to resist all of the components than for single protein. Figure 5a shows the nonspecific adsorption from such natural samples onto HA-Au surfaces. The nonspecific adsorption from soybean milk, cow milk, and undiluted orange juice were 0.6, 9.8, and 16.1 ng/cm^2, respectively. HA-Au surfaces demonstrated a low protein adsorption in these natural complex media, especially from soybean milk where an ultra low protein adsorption (<5 ng/cm^2) could be achieved. Supporting Information Table S2 summarizes the antifouing surfaces and their corresponding protein adsorptions. The antifouling performance of HA-Au surfaces is comparable to or even better than some other antifouling materials, such as the dextran (~6 ng/cm^2 from 0.1 mg/mL BSA solution[44]), and poly-[(methacrylic acid)-*ran*-(2-methacryloyloxyethyl phosphoryl-choline)] (~30 mdeg from 0.1 mg/mL BSA solution[45]).). These results can be attributed to the strong surface hydration derived from hydrophilic groups present in HA chains. Previous studies have also demonstrated that HA has a high refractive index of HA (n = 1.46),[33] providing a high water content on surfaces capable of resisting protein adsorption.[46]

Nonspecific Protein Adsorption on Anti-BSA/HA Surfaces. Besides antifouling performance for SPR biosensors, HA matrix also provides perfect compatibility to bioactive recognition molecules with high immobilization capacity. In this study, we chose anti-BSA as the target recognition molecule to characterize the antifouling and sensor performance of anti-BSA/HA chips. In view of the high content of carboxyl groups present in HA, we used EDC/NHS to activate the carboxyl groups and then covalently attached anti-BSA (1 mg/mL) to HA-Au surfaces via immersion for 30 min. To detect the anti-BSA content, we followed the SPR angle shift after anti-BSA immobilization. On the basis of the angle shift of 0.9° (Figure 6), the immobilization content of anti-BSA is

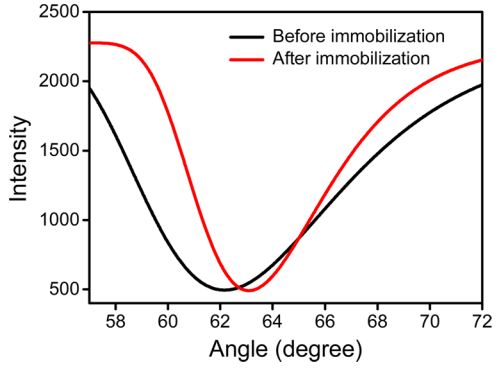

Figure 6. SPR angle shift before (black line) and after (red line) the anti-BSA immobilization.

approximately 780 ng/cm^2, which is higher than (or comparable to) the reported values in the literature.[27,47] High immobilization capacity can be attributed to the 3D structure of HA layer formed by flexible HA chains, as well as the high content of carboxyl groups.

To evaluate the antifouling performance of HA-Au chip for SPR sensing, we measured the nonspecific protein adsorption onto anti-BSA immobilized HA-Au chips. As shown in Supporting Information Figure S5 and Figure 5b, the protein adsorptions from lysozyme and soybean milk were 0.67 and 2.5 ng/cm^2, respectively, indicating that anti-BSA immobilization did not reduce the antifouling ability of HA matrix. For more challenged protein complex including cow milk, 10% blood serum, and undiluted (100%) blood serum, the protein adsorptions increased to 17, 16, and 60 ng/cm^2, respectively. In these cases, the antifouling performance of the anti-BSA/HA surface is still comparable to or even better than that of some other strong hydrophilic surfaces (e.g., ~4 ng/cm^2 lysozyme for poly(ethylene oxide);[7] 62 ng/cm^2 blood plasma for poly(2-hydroxyethyl methacrylate),[28] as shown in Supporting Information Table S2). Additionally, it can be seen that the anti-BSA/HA surface has a lower antifouling ability than the typical zwitterionic surfaces, which should be attributed to the different surface hydration derived from antifouling materials.

Interaction between Anti-BSA and BSA. For practical applications, the sensors are generally used to detect a target molecule in a multicomponent solution. We measured the

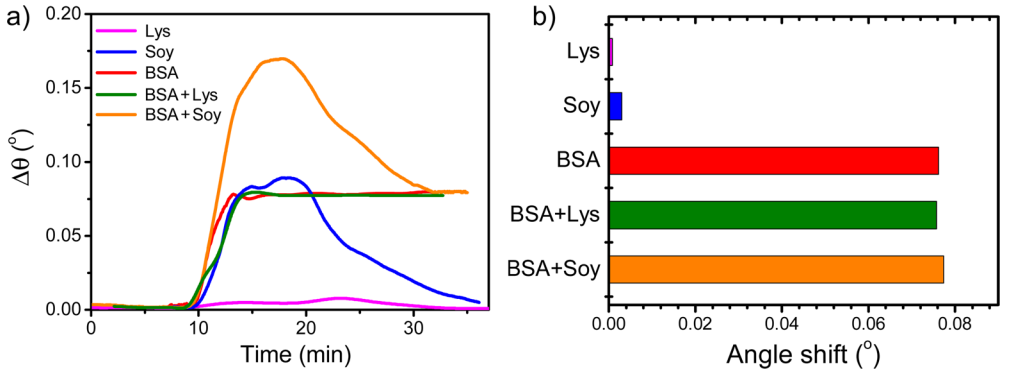

Figure 7. (a) SPR sensorgrams of the interaction of the immobilized anti-BSA on the HA-Au chips with lysozyme (Lys, 1 mg/mL), soybean milk (Soy, ~10 mg/mL), BSA (15 nM), BSA+lysozyme (15 nM, 1 mg/mL, respectively), and BSA+soybean milk (15 nM, 10 mg/mL, respectively). (b) The corresponding SPR angle shifts for the different protein samples.

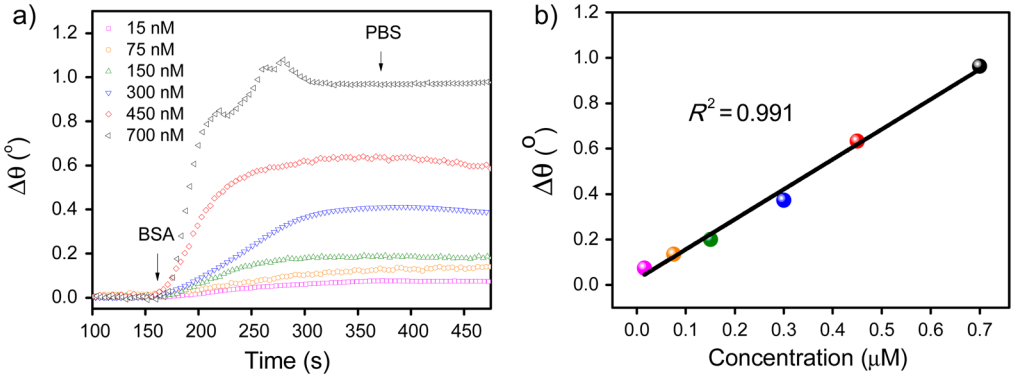

Figure 8. (a) SPR sensorgrams of the interaction of BSA (15−700 nM) with the immobilized anti-BSA in PBS buffer. (b) The calibration curve for the detection of BSA by SPR spectroscopy.

adsorption of reference proteins (lysozyme, soybean milk) on the anti-BSA-immobilized HA surface, and also detected the targeted BSA molecule in the multicomponent solutions including BSA+lysozyme and BSA+soybean milk. As shown in Figure 7, the reference proteins led to a very small SPR angle shift ($\Delta\theta$ = 0.0008 for lysozyme, $\Delta\theta$ = 0.003 for soybean milk), indicating the high selectivity of anti-BSA and good antifouling performance of anti-BSA-immobilized HA layer. The angle shift for single BSA solution is 0.0762, which is very close to that for BSA in lysozyme ($\Delta\theta$ = 0.0757) and soybean milk ($\Delta\theta$ = 0.0774) solutions, respectively. In these cases, the BSA concentration used for dection is 15 nM (~10^{-3} mg/mL). Using lysozyme and soybean milk with high concentrations as reference proteins, the signal-to-noise ratios for 15 nM BSA were 94.6 and 25.8, respectively, suggesting a very high selectivity for BSA sensing.

The real-time SPR angle shift caused by antibody−antigen interaction was recorded with the injection of BSA solution, as shown in Figure 8a. The anti-BSA loaded HA-Au sensor chips demonstrated a satisfactory response to BSA with the concentration range from 15 to 700 nM, which provided direct evidence of high activity of anti-BSA. It also suggested excellent biological compatibility of HA to recognition molecules. As shown in Figure 8b and Supporting Information Figure S6, the corresponding SPR angle shift showed a good linear relationship (R^2 = 0.991) within the concentration range of 15−700 nM. When the BSA concentration was lower than 15 nM or higher than 700 nM, however, the angle shift was not proportional to the change in concentrations. The kinetic parameters for the interaction between BSA and anti-BSA were calculated on the basis of a previously reported method.[48] The association rate constant (k_a), dissociation rate constant (k_d), and equilibrium constant ($K = k_a/k_d$) were 8.49 × 10^4 M^{-1} S^{-1}, 4.17 × 10^{-3} S^{-1}, and 2.03 × 10^7 M^{-1}, respectively. The equilibrium constant is close to that reported in previous studies.[49,50] Additionally, we also investigated the regenerability of anti-BSA sensor chips. In a typical experiment, we injected 100 μL of NaOH (10 mM) into the flow cell to wash away the bound BSA. The baseline then was re-established by PBS solution, followed by injection of BSA for another cycle. As shown in Supporting Information Figure S7, the anti-BSA sensor chip showed a good performance after 4 cycles with a total time of 4 h. Our results demonstrate that HA-Au has great potential as a matrix for the immobilization of bioactive antibody and further quantitative detection of target agents. The minimum response signal ($\Delta\theta$) was about 0.075 at 15 nM, while the maximum response signal was 0.97 at 700 nM.

CONCLUSIONS

In summary, we fabricated a novel protein-resistant surface by covalently grafting HA molecules to Au substrate and demonstrated that the HA-Au and antibody-immobilized HA surfaces exhibited good antifouling performance against the nonspecific adsorption from single protein solutions and complex media. An ultralow or low protein adsorption on these surfaces was achieved from single protein solutions, food protein complex, and 10% blood serum, which can be attributed to their strong hydration and extreme hydrophilicity

(contact angle of 12°) resulting from high content of carboxyl and amide groups. The HA matrix also allowed high immobilization capacity of 780 ng/cm^2 for bioactive anti-BSA molecules. The anti-BSA loaded HA-Au chips displayed high selectivity and sensitivity to BSA in complex solutions, suggesting the good stability and compatibility of an HA matrix to biological recognition molecules. In view of the low cost and ease of availability of natural HA molecules, combined with the excellent antifouling performance, high immobilization capacity, and biocompatibility demonstrated in this study, HA has great potential as a matrix for the fabrication of antifouling surfaces and SPR biosensor chips.

■ ASSOCIATED CONTENT

Ⓢ Supporting Information

AFM image of the scratched HA-Au surface, SPR angle scanning spectra before and after protein adsorption on various surfaces, SPR sensorgrams showing the nonspecific protein adsorption from various media onto HA-Au surfaces, SPR angle scanning spectra before and after protein adsorption onto HA-Au surfaces from various media, SPR sensorgrams showing the nonspecific protein adsorption onto anti-BSA immobilized HA-Au surfaces, detection of BSA in SPR spectroscopy over a concentration range from 0.1 nM to 2.5 μM, SPR sensorgram showing the regeneration of anti-BSA loaded HA-Au sensor chips using a 10 mM NaOH solution, static water contact angles of the bare Au, SAM, and HA-Au surfaces, and summary of the antifouling surface and the corresponding nonspecific protein adsorption. This material is available free of charge via the Internet at http://pubs.acs.org.

■ AUTHOR INFORMATION

Corresponding Authors

*Tel.: +86 22 27407799. Fax: +86 22 27407599. E-mail: tjuhrl@tju.edu.cn.
*E-mail: surx@tju.edu.cn.

Notes

The authors declare no competing financial interest.

■ ACKNOWLEDGMENTS

This work was supported by the Ministry of Science and Technology of China (Grants 2012YQ090194, 2012AA06A303, and 2012BAD29B05), the Natural Science Foundation of China (Grants 21276192 and 21306134), and the Ministry of Education (Grants B06006 and NCET-11-0372). We are grateful to Prof. Jacob Israelachvili, Mrs. Nancy Emerson, and Mr. Jeffrey Scott at the University of California, Santa Barbara, for their helpful corrections to the English writing.

■ REFERENCES

(1) Homola, J.; Yee, S. S.; Gauglitz, G. Surface Plasmon Resonance Sensors: Review. *Sens. Actuators, B* **1999**, *54*, 3−15.
(2) Hutter, E.; Fendler, J. H. Exploitation of Localized Surface Plasmon Resonance. *Adv. Mater.* **2004**, *16*, 1685−1706.
(3) Homola, J. Surface Plasmon Resonance Sensors for Detection of Chemical and Biological Species. *Chem. Rev.* **2008**, *108*, 462−493.
(4) Mayer, K. M.; Hafner, J. H. Localized Surface Plasmon Resonance Sensors. *Chem. Rev.* **2011**, *111*, 3828−3857.
(5) Zeng, S.; Baillargeat, D.; Ho, H.-P.; Yong, K.-T. Nanomaterials Enhanced Surface Plasmon Resonance for Biological and Chemical Sensing Applications. *Chem. Soc. Rev.* **2014**, *43*, 3426−3452.
(6) Vaisocherová, H.; Yang, W.; Zhang, Z.; Cao, Z.; Cheng, G.; Piliarik, M.; Homola, J.; Jiang, S. Ultralow Fouling and Functionalizable Surface Chemistry Based on A Zwitterionic Polymer Enabling Sensitive and Specific Protein Detection in Undiluted Blood Plasma. *Anal. Chem.* **2008**, *80*, 7894−7901.
(7) Pop-Georgievski, O.; Verreault, D.; Diesner, M. O.; Proks, V.; Heissler, S.; Rypacek, F.; Koelsch, P. Nonfouling Poly(Ethylene Oxide) Layers End-Tethered to Polydopamine. *Langmuir* **2012**, *28*, 14273−14283.
(8) Adkins, J. N. Toward a Human Blood Serum Proteome: Analysis by Multidimensional Separation Coupled with Mass Spectrometry. *Mol. Cell. Proteomics* **2002**, *1*, 947−955.
(9) Choi, S.; Chae, J. Methods of Reducing Non-Specific Adsorption in Microfluidic Biosensors. *J. Micromech. Microeng.* **2010**, *20*, 075015.
(10) Blaszykowski, C.; Sheikh, S.; Thompson, M. Surface Chemistry to Minimize Fouling from Blood-Based Fluids. *Chem. Soc. Rev.* **2012**, *41*, 5599−5612.
(11) Prime, K. L.; Whitesides, G. M. Adsorption of Proteins onto Surfaces Containing End-Attached Oligo(Ethylene Oxide): A Model System Using Self-Assembled Monolayers. *J. Am. Chem. Soc.* **1993**, *115*, 10714−10721.
(12) Harder, P.; Grunze, M.; Dahint, R.; Whitesides, G. M.; Laibinis, P. E. Molecular Conformation in Oligo(Ethylene Glycol)-Terminated Self-Assembled Monolayers on Gold and Silver Surfaces Determines Their Ability to Resist Protein Adsorption. *J. Phys. Chem. B* **1998**, *102*, 426−436.
(13) Ma, H.; Wells, M.; Beebe, T. P.; Chilkoti, A. Surface-Initiated Atom Transfer Radical Polymerization of Oligo(Ethylene Glycol) Methyl Methacrylate from a Mixed Self-Assembled Monolayer on Gold. *Adv. Funct. Mater.* **2006**, *16*, 640−648.
(14) Ostuni, E.; Chapman, R. G.; Holmlin, R. E.; Takayama, S.; Whitesides, G. M. A Survey of Structure-Property Relationships of Surfaces That Resist The Adsorption of Protein. *Langmuir* **2001**, *17*, 5605−5620.
(15) Sileika, T. S.; Kim, H. D.; Maniak, P.; Messersmith, P. B. Antibacterial Performance of Polydopamine-Modified Polymer Surfaces Containing Passive and Active Components. *ACS Appl. Mater. Interfaces* **2011**, *3*, 4602−4610.
(16) Jiang, J. H.; Zhu, L. P.; Zhu, L. J.; Zhang, H. T.; Zhu, B. K.; Xu, Y. Y. Antifouling and Antimicrobial Polymer Membranes Based on Bioinspired Polydopamine and Strong Hydrogen-Bonded Poly(*N*-Vinyl Pyrrolidone). *ACS Appl. Mater. Interfaces* **2013**, *5*, 12895−12904.
(17) Frazier, R.; Matthijs, G.; Davies, M.; Roberts, C.; Schacht, E.; Tendler, S. Characterization of Protein-Resistant Dextran Monolayers. *Biomaterials* **2000**, *21*, 957−966.
(18) Ederth, T.; Ekblad, T.; Pettitt, M. E.; Conlan, S. L.; Du, C. X.; Callow, M. E.; Callow, J. A.; Mutton, R.; Clare, A. S.; D'Souza, F.; Donnelly, G.; Bruin, A.; Willemsen, P. R.; Su, X. J.; Wang, S.; Zhao, Q.; Hederos, M.; Konradsson, P.; Liedberg, B. Resistance of Galactoside-Terminated Alkanethiol Self-Assembled Monolayers to Marine Fouling Organisms. *ACS Appl. Mater. Interfaces* **2011**, *3*, 3890−3901.
(19) Fyrner, T.; Lee, H.-H.; Mangone, A.; Ekblad, T.; Pettitt, M. E.; Callow, M. E.; Callow, J. A.; Conlan, S. L.; Mutton, R.; Clare, A. S. Saccharide-Functionalized Alkanethiols for Fouling-Resistant Self-Assembled Monolayers: Synthesis, Monolayer Properties, and Antifouling Behavior. *Langmuir* **2011**, *27*, 15034−15047.
(20) Lin, S.; Zhang, B.; Skoumal, M. J.; Ramunno, B.; Li, X.; Wesdemiotis, C.; Liu, L.; Jia, L. Antifouling Poly(beta-Peptoid)s. *Biomacromolecules* **2011**, *12*, 2573−2582.
(21) Ham, H. O.; Park, S. H.; Kurutz, J. W.; Szleifer, I. G.; Messersmith, P. B. Antifouling Glycocalyx-Mimetic Peptoids. *J. Am. Chem. Soc.* **2013**, *135*, 13015−13022.
(22) Jiang, S.; Cao, Z. Ultralow-Fouling, Functionalizable, and Hydrolyzable Zwitterionic Materials and Their Derivatives for Biological Applications. *Adv. Mater.* **2010**, *22*, 920−932.
(23) Li, G.; Cheng, G.; Xue, H.; Chen, S.; Zhang, F.; Jiang, S. Ultra Low Fouling Zwitterionic Polymers with a Biomimetic Adhesive Group. *Biomaterials* **2008**, *29*, 4592−4597.

(24) Zhao, C.; Li, L.; Wang, Q.; Yu, Q.; Zheng, J. Effect of Film Thickness on The Antifouling Performance of Poly(Hydroxy-Functional Methacrylates) Grafted Surfaces. *Langmuir* **2011**, *27*, 4906−4913.
(25) Mi, L.; Jiang, S. Integrated Antimicrobial and Nonfouling Zwitterionic Polymers. *Angew. Chem., Int. Ed.* **2014**, *53*, 1746−1754.
(26) Cao, Z. Q.; Jiang, S. Y. Super-Hydrophilic Zwitterionic Poly(Carboxybetaine) and Amphiphilic Non-Ionic Poly(Ethylene Glycol) for Stealth Nanoparticles. *Nano Today* **2012**, *7*, 404−413.
(27) Huang, C. J.; Li, Y.; Jiang, S. Zwitterionic Polymer-Based Platform with Two-Layer Architecture for Ultra Low Fouling and High Protein Loading. *Anal. Chem.* **2012**, *84*, 3440−3445.
(28) Vaisocherová, H.; Ševců, V.; Adam, P.; Špačková, B.; Hegnerová, K.; de los Santos Pereira, A.; Rodriguez-Emmenegger, C.; Riedel, T.; Houska, M.; Brynda, E.; Homola, J. Functionalized Ultra-Low Fouling Carboxy- and Hydroxy-Functional Surface Platforms: Functionalization Capacity, Biorecognition Capability and Resistance to Fouling from Undiluted Biological Media. *Biosens. Bioelectron.* **2014**, *51*, 150−157.
(29) Zhao, Z. L.; Ni, H. G.; Han, Z. Y.; Jiang, T. F.; Xu, Y. J.; Lu, X. L.; Ye, P. Effect of Surface Compositional Heterogeneities and Microphase Segregation of Fluorinated Amphiphilic Copolymers on Antifouling Performance. *ACS Appl. Mater. Interfaces* **2013**, *5*, 7808−7818.
(30) Amadei, C. A.; Yang, R.; Chiesa, M.; Gleason, K. K.; Santos, S. Revealing Amphiphilic Nanodomains of Anti-Biofouling Polymer Coatings. *ACS Appl. Mater. Interfaces* **2014**, *6*, 4705−4712.
(31) Yoshioka, T.; Tsuru, K.; Hayakawa, S.; Osaka, A. Preparation of Alginic Acid Layers on Stainless-Steel Substrates for Biomedical Applications. *Biomaterials* **2003**, *24*, 2889−2894.
(32) Cao, B.; Li, L.; Wu, H.; Tang, Q.; Sun, B.; Dong, H.; Zhe, J.; Cheng, G. Zwitteration of Dextran: A Facile Route to Integrate Antifouling, Switchability and Optical Transparency into Natural Polymers. *Chem. Commun.* **2014**, *50*, 3234−3237.
(33) Suh, K. Y.; Yang, J. M.; Khademhosseini, A.; Berry, D.; Tran, T. N.; Park, H.; Langer, R. Characterization of Chemisorbed Hyaluronic Acid Directly Immobilized on Solid Substrates. *J. Biomed. Mater. Res., Part B* **2005**, *72*, 292−298.
(34) Ombelli, M.; Costello, L.; Postle, C.; Anantharaman, V.; Meng, Q. C.; Composto, R. J.; Eckmann, D. M. Competitive Protein Adsorption on Polysaccharide and Hyaluronate Modified Surfaces. *Biofouling* **2011**, *27*, 505−518.
(35) Prime, K.; Whitesides, G. Self-Assembled Organic Monolayers: Model Systems for Studying Adsorption of Proteins at Surfaces. *Science* **1991**, *252*, 1164−1167.
(36) Bauer, S.; Arpa-Sancet, M. P.; Finlay, J. A.; Callow, M. E.; Callow, J. A.; Rosenhahn, A. Adhesion of Marine Fouling Organisms on Hydrophilic and Amphiphilic Polysaccharides. *Langmuir* **2013**, *29*, 4039−4047.
(37) Stenberg, E.; Persson, B.; Roos, H.; Urbaniczky, C. Quantitative Determination of Surface Concentration of Protein with Surface Plasmon Resonance Using Radiolabeled Proteins. *J. Colloid Interface Sci.* **1991**, *143*, 513−526.
(38) Azzaroni, O.; Brown, A. A.; Huck, W. T. S. UCST Wetting Transitions of Polyzwitterionic Brushes Driven by Self-Association. *Angew. Chem., Int. Ed.* **2006**, *45*, 1770−1774.
(39) Zhao, J.; Shi, Q.; Luan, S.; Song, L.; Yang, H.; Shi, H.; Jin, J.; Li, X.; Yin, J.; Stagnaro, P. Improved Biocompatibility and Antifouling Property of Polypropylene Non-Woven Fabric Membrane by Surface Grafting Zwitterionic Polymer. *J. Membr. Sci.* **2011**, *369*, 5−12.
(40) Ma, H.; Hyun, J.; Stiller, P.; Chilkoti, A. Non-Fouling Oligo(Ethylene Glycol)- Functionalized Polymer Brushes Synthesized by Surface-Initiated Atom Transfer Radical Polymerization. *Adv. Mater.* **2004**, *16*, 338−341.
(41) Tischer, T.; Claus, T. K.; Bruns, M.; Trouillet, V.; Linkert, K.; Rodriguez-Emmenegger, C.; Goldmann, A. S.; Perrier, S.; Borner, H. G.; Barner-Kowollik, C. Spatially Controlled Photochemical Peptide and Polymer Conjugation on Biosurfaces. *Biomacromolecules* **2013**, *14*, 4340−4350.
(42) Liu, Q.; Singh, A.; Lalani, R.; Liu, L. Ultralow Fouling Polyacrylamide on Gold Surfaces Via Surface-Initiated Atom Transfer Radical Polymerization. *Biomacromolecules* **2012**, *13*, 1086−1092.
(43) Liu, Q.; Singh, A.; Liu, L. Amino Acid-Based Zwitterionic Poly(Serine Methacrylate) As an Antifouling Material. *Biomacromolecules* **2013**, *14*, 226−231.
(44) Uchida, K.; Hoshino, Y.; Tamura, A.; Yoshimoto, K.; Kojima, S.; Yamashita, K.; Yamanaka, I.; Otsuka, H.; Kataoka, K.; Nagasaki, Y. Creation of a Mixed Poly(Ethylene Glycol) Tethered-Chain Surface for Preventing The Nonspecific Adsorption of Proteins And Peptides. *Biointerphases* **2007**, *2*, 126−130.
(45) Akkahat, P.; Kiatkamjornwong, S.; Yusa, S.-i.; Hoven, V. P.; Iwasaki, Y. Development of a Novel Antifouling Platform for Biosensing Probe Immobilization from Methacryloyloxyethyl Phosphorylcholine-Containing Copolymer Brushes. *Langmuir* **2012**, *28*, 5872−5881.
(46) Brault, N. D.; Sundaram, H. S.; Li, Y.; Huang, C. J.; Yu, Q.; Jiang, S. Dry Film Refractive Index As an Important Parameter for Ultra-Low Fouling Surface Coatings. *Biomacromolecules* **2012**, *13*, 589−593.
(47) Yang, W.; Xue, H.; Li, W.; Zhang, J.; Jiang, S. Pursuing "Zero" Protein Adsorption of Poly(Carboxybetaine) from Undiluted Blood Serum and Plasma. *Langmuir* **2009**, *25*, 11911−11916.
(48) Chang, T.-C.; Wu, C.-C.; Wang, S.-C.; Chau, L.-K.; Hsieh, W.-H. Using a Fiber Optic Particle Plasmon Resonance Biosensor to Determine Kinetic Constants of Antigen−Antibody Binding Reaction. *Anal. Chem.* **2012**, *85*, 245−250.
(49) Li, G.; Zhou, X.; Wang, Y.; El-Shafey, A.; L. Chiu, N. H.; Krull, I. S. Capillary Isoelectric Focusing and Affinity Capillary Electrophoresis Approaches for The Determination of Binding Constants for Antibodies to The Prion Protein. *J. Chromatogr., A* **2004**, *1053*, 253−262.
(50) Li, B.; Chen, J.; Long, M. Measuring Binding Kinetics of Surface-Bound Molecules Using The Surface Plasmon Resonance Technique. *Anal. Biochem.* **2008**, *377*, 195−201.